A REVIEW OF PUBLIC GEOPHYSICAL DATA KILAUEA - EAST RIFT AREA HAWAII

prepared for

THERMAL POWER COMPANY
601 CALIFORNIA STREET
SAN FRANCISCO, CALIFORNIA

by

HOWARD P. ROSS, PH.D.
Geophysical Consultant
Salt Lake City, Utah

NOVEMBER 1982

A REVIEW OF PUBLIC GEOPHYSICAL DATA KILAUEA - EAST RIFT AREA HAWAII

by

Howard P. Ross, Ph.D.
Geophysical Consultant

for

THERMAL POWER COMPANY
Geothermal Division
SAN FRANCISCO, CALIFORNIA

CONTENTS

ILLUSTRATIONS

Figures

INTRODUCTION

The Hawaii Institute of Geophysics (HIG), the Colorado School of Mines, the U. S. Geological Survey (USGS) and other groups carried out an extensive and varied exploration program in the Kileaua east rift zone on the island of Hawaii between 1973 and 1980. This program made widespread use of goephysical techniques to determine the subsurface structure of the east rift zone and identified a potential geothermal reservoir in the Puna District. The successful drilling of geothermal well HGP-A by the Hawaii Institute of Geophysics in 1976 proved the validity of geophysical interpretations and established the Puna geothermal resource as one of the hottest proven geothermal systems. Subsequent drilling by Thermal Power Company and its associates has resulted in two more potential producing wells.

Thermal Power Company is currently evaluating the overall geothermal potential of the Puna reservoir and nearby areas in the east rift zone. Thermal Power Company has thus engaged Howard Ross as a consultant in exploration geophysics to provide a generalized compilation of the public geophysical data, to provide an outside evaluation of the various data sets, and to complete an integrated interpretation of these data. This report presents the data compilation, data evaluation, interpretation and recommendations for further work. Additional assignments such as the design and procurement of additional geophysical surveys, and review of proprietary data sets are not addressed in this report. The Earth Science Laboratory, University of Utah Research Institute (ESL/UURI) has provided drafting, library, secretarial, and additional interpretative services to Howard Ross under a subcontract.

The compilation and interpretation presented here represents a reasonable

compromise between completeness, interpretative effort, cost to Thermal Power Company, and the schedule of the client's program. Additional interpretation could always be done with the data at hand. Realistically, the geophysical data reviewed represent well over ten man years of survey design, data acquisition and data interpretation and a much greater background of geologic familiarity. Accordingly only selected areas have received new data interpretation, though essentially all pre-existing interpretations have been reviewed. The mechanics of completing the data compilation have provided the familarity with the data and the geology to move ahead with an in depth data review and integrated interpretation.

GEOLOGY

A voluminous literature describes various aspects of the geology, petrology, volcanic and tectonic setting of the island of Hawaii and the Kilauea east rift zone. A detailed review of these data is beyond the scope of the present study. It is useful however to include a general description of the geologic setting as a background to later geophysical discussions.

Kilauea Volcano is the southeasternmost shield volcano in the Hawaiian-Emperor chain of islands. Kilauea, situated on the east flank of Mauna Loa, (Figure 1) and Mauna Loa itself, are among the most active volcanoes on earth (Swanson et al., 1976). The east rift extends from Kilauea southeastward for 7.3 km, then trends N65°E past Cape Kamukahi where it can be traced by bathymetry for approximately 70 km (Moore, 1971). The geology of the entire eastern portion of the island of Hawaii is dominated by a great sequence of seaward dipping lava flows which emanate from Mauna Loa and Kilauea Volcanoes. The younger flows fill in earlier vents and flow features and obscure older faults, fissures, and entire flow systems. Geologic studies by

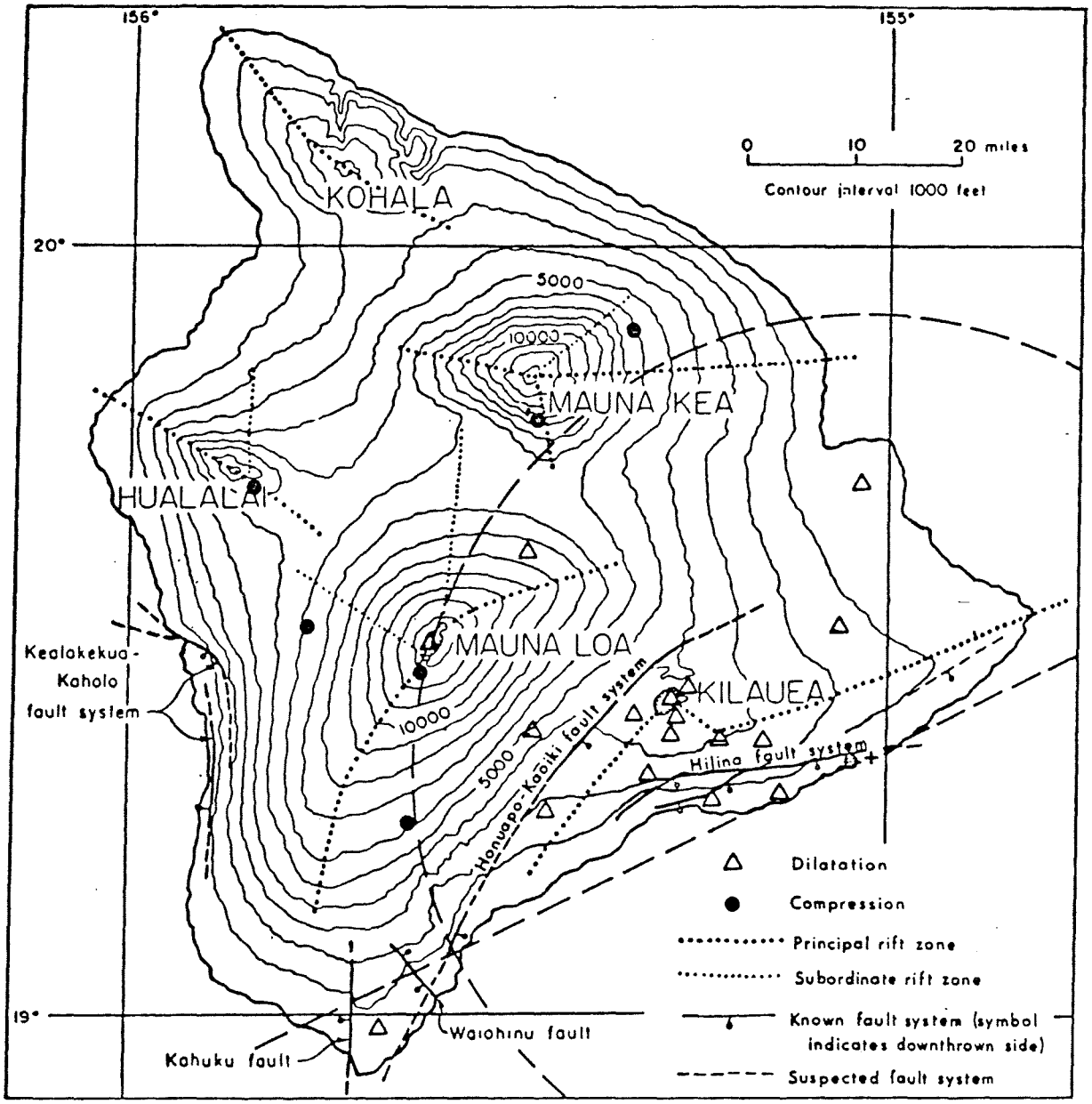

Fig. 1. Generalized location map showing major geologic features in relation to the Kilauea east rift zone. The distribution of dilations and compressions as determined by the seismic stations of the Hawaiian Volcano Observatory are also indicated. (From Furumoto and Kovach, 1979).

Peterson (1967), and Moore (1971) indicate the geologic structure and extent of historical flows in the Kilauea and east rift areas. Holcomb (1980) and Moore (1982) present detailed geologic mapping of lava flows, fissures and faulting for the Kilauea and east rift zones. The principal geologic features of Holcomb's (1980) map, reduced to 1:100,000 scale, is presented as Plate I of this report. The petrography of the volcanic rocks is described by Macdonald (1949) who noted that the lavas of Mauna Loa and Kilaueau Volcanoes are predominantly olivine basalt with smaller proportions of basalt.

The subsurface structure and tectonic setting of the east rift area, of prime importance to the evaluation of geothermal resource potential, has been studied through integrated geologic, seismic and gravity studies (Furumoto and Kovach, 1979; Swanson et al., 1976). Seismic evidence in particular indicates that the southeast side of the rift zone is being displaced seaward by the intrusion of magma as dikes within the rift zone. The dikes are believed to be individually thin, a few meters wide, and to be nearly vertical or to dip steeply southward (Swanson et al., 1976). The north flank of the rift zone is relatively immobile and less seismically active. This results from the buttressed position of Kilauea and the rift zone itself, against the stable south flank of the massive Mauna Loa shield volcano, in marked contrast to the unbounded south flank. Swanson et al. (1976) suggest that the active seaward side of the rift zone has probably migrated several kilometers eastward in recent time. Triangulation, trilateration and leveling data indicate the south flank of Kilauea has been displaced upward and away from the rift zone by several meters during the 20th century alone. Keller et al. (1977) point out that grabens bounding the rift zone have been filled repeatedly, making vertical movement within the graben difficult to measure.

The high rainfall in the eastern Hawaii area (100-200 inches/yr) produces ground waters which move readily through the porous and permeable basalts and move down dip relatively unimpeded until ponded by the dikes and structures of the east rift zone (Fig. 2). Thus a typical Ghyben-Herzberg system probably is not present in the east rift area of Hawaii (Keller et al., 1977). Both electrical resistivity data and drill results indicate salt water close to sea level in the Puna area.

The principal faults, fissures and caldera features of the east rift zone (Holcomb, 1980) are shown in Plate I which is intended to serve as a simplified geologic base map for this report. The details of the flow sequences have been omitted since they seem to bear little detailed relationship to the geophysical data at this scale.

GEOPHYSICS

An extensive geophysical data base has been developed since 1973 as part of the east rift zone geothermal exploration program. Many data sets have been reported in preliminary form (i.e. thesis form), summarized by other authors, included in integrated interpretations and later reinterpreted. Certain data bases have been extended more recently. This situation has complicated the data compilation and interpretation. We beleive that no significant published data has been omitted from the compilation included in Plates II-VIII, although some data has been omitted for clarity when it does not significantly enhance the data base. The data reviewed to date and included in the interpretation are listed in Table 1.

Thermal Methods Data

Furumoto (1978) describes the use of airborne infrared surveys early in

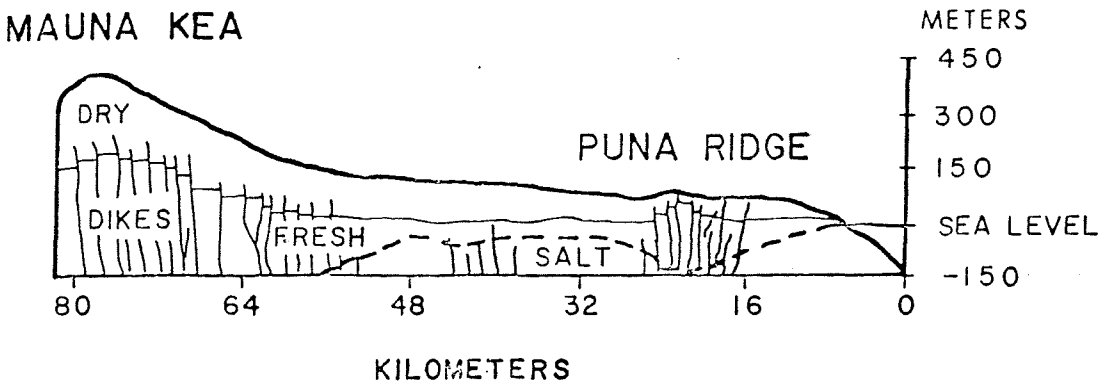

Figure 2a Generalized cross-section from Mauna Kea to the Puna Ridge showing fresh and salt-water distribution (after Stearns and Macdonald, 1946, p. 225).

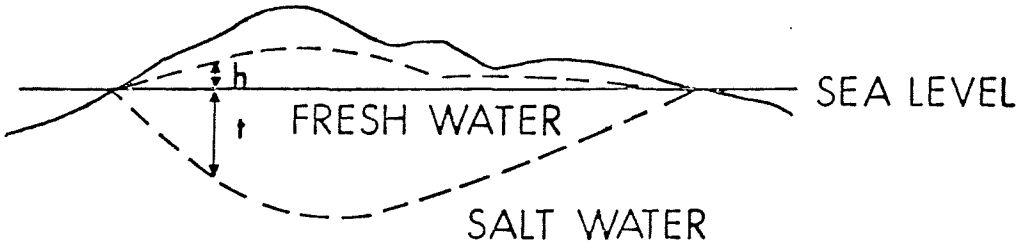

Figure 2b The Ghyben-Herzberg Principle showing the lens of fresh water depressed below sea level (after Stearns, 1966, p. 234).

Figures 2a and 2b taken from Keller et al., 1977.

Table 1

Geophysical Data Reviewed

Thermal Data	Description
Furumoto (1978)	Airborne infrared surveys
Kauahikaua & Klein (1977)	Well and spring temperature compilation
Hawaii Institute of Geophysics-NOAA (1982)	Well and spring temperature compilation
Epp and Halunen (1979)	Well temperature profiles
Gravity Data	
Kinoshita et al. (1963)	Regional Bouguer gravity map of Hawaii
Krivoy and Eaton (1961)	Kilauea and east rift surveys
Furumoto et al. (1976)	Detailed survey, east rift zone
Broyles et al. (1979)	Two dimensional model interpretation
Magnetic Data	
Thomas et al. (1979)	Total Force magnetic map of Hawaii (1965)
Malahoff and Woollard (1968)	Total Force magnetic map of Hawaii (1965)
Godson et al. (1981)	Aeromagnetic map of Hawaii (1978)
Furumoto (1978)	Qualitative magnetic interpretation
Electrical Data	
Keller et al. (1977)	Summary HIG report on electrical studies
Keller et al. (1977).	Reconnaissance dipole mapping surveys
Keller et al. (1977)	Resistivity sectioning surveys
Keller et al. (1977); Skokan (1974)	Time-domain electromagnetic (TDEM) survey
Kauahikaua and Klein (1977)	Electromagnetic induction sounding measurements
Kauahikaua and Klein (1977)	Electromagnetic transient soundings (EMTS)
Kauahikaua (1981)	Interpretation of above EMTS
Kauahikaua and Klein (1978)	Integrated interpretation near HPG-A
Kauahikaua et al. (1980)	Mise-a-la-masse from HGP-A
Zablocki (1977)	Self-potential survey, east Puna area
Zablocki (1976)	Self-potential survey, Kilauea Volcano
Rudman (1978)	Analysis of HGP-A goephysical logs
Seismic Data	
USGS Periodic Reports (1960-1980)	Quarterly and annual reports of earthquakes
Suyenaga et al. (1978)	HIG summary report on seismic studies
Suyenaga and Furumoto (1978)	Earthquake epicenter summary, 1964-1973
Suyenaga and Furumoto (1978)	7-seismometer microearthquake survey
Mattice and Furumoto (1978)	2-seismometer microearthquake survey
Norris and Furumoto (1978)	Seismic ground noise survey
Suyenaga (1978)	Shallow seismic refraction survey
Broyles and Furumoto (1977)	Crustal refraction survey
Furumoto (1978)	Integrated interpretation of seismic data
Thomas et al. (1978)	Integrated data summary

the exploration program to identify near surface thermal anomalies, thermal seeps, etc. The subsequent electrical surveys were conducted in part as follow up on the results of these reconnaissance infrared surveys. Kauahikaua and Klein (1977) presented a useful summary of well temperatures and coastal spring temperatures, and this has been included in Plate I as a thermal base map for comparison with other geophysical data. The data are too sparse and complex to justify a contoured map of thermal gradients or heat flow. Although the data base is too limited to define a pattern, we note: a trend of cool wells north of the rift zone (9-5, 9-11) and possibly east of Kapoho Crater (well 1-very shallow); several warm-to-hot wells along the central portion of the rift zone (wells I, II, III, IV, HGP-A); and warm wells (9-9, Allison) and coastal springs south of the active rift zone, but north and east of Kamaili. Steaming fissures above the dike complex further testify to high temperatures along parts of the central portion of the rift zone. Correlations with gravity and magnetic data, yet to be discussed, indicate a probability for north-south oriented structures which may cut the dike complex and permit the southward migration of high temperature fluids. Alternatively these structures could themselves be conduits for a separate geothermal reservoir oriented perpendicular to and south of the rift zone. Many of the warm wells occur within or near self-potential anomalies but few of the background temperature wells do. Some wells were sited specifically on the self-potential anomalies, however.

Epp and Halunen (1979) describe the measurement problems and temperature profiles for several wells in the Puna rift area. They note that temperatures decrease rapidly to the north and south of the rift zone. Wells III (GTW-3), 9-9, and Allison show decreasing temperatures at the bottom of the hole, which is below sea level, suggesting that the hottest water passed through a high-

temperature region upslope from these wells.

Gravity Data

Several gravity studies have been completed for portions of the island of Hawaii since 1960. Kinoshita et al. (1963) published a Bouguer Gravity Anomaly Map for the entire island which incorporated earlier local surveys near Kilauea and its major rift zones (Krivoy and Eaton, 1961). This map provides the regional coverage for our integrated gravity map, Plate II. The regional data base contributes approximately 50 stations in the East Rift Area, and each of these have been precisely located. The actual Bouguer gravity values are reproduced from Krivoy and Eaton (1961).

Furumoto et al. (1976) completed a detailed gravity survey of the east rift area in support of the HIG geothermal project during 1975. This survey represents the most detailed gravity data made public, and includes 210 stations in approximately 150 km^2, at a basic grid spacing of 0.5 km. These data show small deviations from the earlier regional survey Plate II, and are included as a detailed overlay to the regional data. Only the contoured data, not individual station locations and data values, were available for study.

Broyles et al. (1979) have computed a series of two dimensional models which match the higher frequency portion of two gravity profiles from the detailed data set, and illustrate the wide range of ambiguity which can result from interpretation of these data. Their interpretation was strongly constrained by seismic data. We have reviewed existing interpretations of the gravity data and undertaken additional qualitative and numerical model studies. The strong correlation between Bouguer gravity and topography (elevation) of the entire eastern portion of Hawaii causes us to question the density of 2.3 gm/cm^3 (too low?) used in the Bouguer correction, as discussed

earlier by Kinoshita et al. (1963). In addition there is uncertainty about the regional gradient since only the high frequency portion of the gravity anomaly has been adequately defined. Our numerical models for a shallow (0-2 km), narrow (3-5 km wide) dike with density contrast 0.4 g/cc or larger show a well defined anomaly as compared to the observed data. Various combinations of a narrow (3-5 km) shallow body merging with a wider body (but probably less than 12 km wide) at depth will match the observed data. Thus a detailed reinterpretation of the gravity data will contribute little to the definition of the dike complex and would be subject to considerable ambiguity.

A qualitative interpretation of the detailed gravity data clearly shows a displacement to the north for the gravity anomaly crest between HGP-A and Cape Kumukahi. The crest of the anomaly also appears smoother to the east, implying greater depth to the top of the dike complex. This leads to our qualitative interpretation of a major north-south structure very near to the reservoir site as shown on Plate II. The position of this hypothesized structure would include the north-trending self-potential anomaly C and agree with north-south discontinuities in the magnetic data (which are poorly defined due to the 1.6 km line spacing). The indication of this structural discontinuity is the main contribution of the gravity data at the prospect-exploration scale.

Magnetic Data

Several aeromagnetic surveys have been conducted over the island of Hawaii in an attempt to define the deep structure of the volcanic systems (Thomas et al., 1979). Malakoff and Wollard (1968) completed a high altitude reconnaissance survey of the entire island in 1965. The high altitudes, 12,000 to 14,000 feet barometric elevation, were appropriate for identifying

larger and deeper (5-10 Km) structural features but show relatively little agreement with mapped structure. The east rift zone does appear as a weakly defined magnetic high on this survey. Furumoto (1978) suggests that, based on a (linear) temperature extrapolation from well HGP-1, the dike complex should be hot enough to be above the Curie temperature ($\sim$580°C) at depth, and thus should be nonmagnetic. Furumoto's regional magnetic model does support the presence of nonmagnetic material in the area of the dike complex at depths greater than 2.4 km below sea level. The disagreement between his model results and the observed data, and the regional nature of his analysis make his study of limited value at the present stage of the geothermal exploration program.

Furumoto (1976) also reports the interpretation of a single ground magnetic traverse between Kaimu and Pahoa which is part of a more complete ground magnetic survey. The noisy ground magnetic data required filtering prior to interpretation. His model of this profile led to the interpretation that only the southern portion of the dike complex was nonmagnetic and thus above the Curie point, and that some portions of the non dike rocks are hot. Other traverses showed that not all of the dike complex was nonmagnetic. The interpretation that all nonmagnetic rocks are above the Curie point may be incorrect and misleading, and probably really indicates a much more complex structure within the rift area or dike complex.

Godson et al. (1981) published a more detailed aeromagnetic map of Hawaii which is the basis of our study to date. These data were acquired in March 1978 at an average elevation of 300 m above the ground. The low level gives an appropriate amount of near surface detail but the line spacing of 1.6 km (1 mi.) was quite wide. The flight line direction was north-south. The data

were presented at a scale of 1:250,000 in colored format which did not permit detailed interpretation. The map scale was expanded to 1:100,000 and the values recontoured to permit overlay use with other data sets and is presented as our Plate III. The north-south elongation of magnetic contours along flight lines may be due in part to varying terrain clearance or flight path recovery problems.

Although the line spacing of this survey (1.6 km) is reconnaissance in nature, the data clearly indicate several different magnetic sources in the region of the dike complex. The geometries of these magnetic sources relate to major structures, and perhaps to temperature, at depth. An iterative model solution has been completed to determine the magnetic source geometries and apparent magnetizations which give rise to the magnetic contours. The program used calculates the net magnetic field of a large number of vertically sided prisms of different magnetizations. Plate IIIB shows the specific model geometries for the Puna area model. The model input parameters are included as Appendix II. There are significant differences between the computed magnetic contours and the observed data, especially near the steep negative gradient north of Pahoa. Nonetheless, the model provides a good match to most of the magnetic features in the east rift-Pahoa area. The model data provides a basis for the more complete mapping of magnetic sources shown on Plate VIII.

Without terrain clearance records and more detailed data one should not place great importance on the interpreted magnetizations, depths, or depth extents. A minimum information assumption that all bodies are magnetic to depths of 5 km indicates a substantial variation in apparent susceptibility, from 0 to 10,000 μcgs. This is truly just an "apparent" or relative susceptibility and does not account for background values or a remanent

magnetism component (which is probably present, but close to the direction of the present inducing field). The modeling is most useful in defining the source geometries and positions for better correlation with other data sets and for identifying possible geologic structures.

Study of the 1981 data through overlay of known geology, and numerical modeling done to date, indicate the following: 1) The Chain of Craters and lava flow area is positively magnetized (near surface) between Kilauea Crater and Heiheiahulu; 1) the more magnetic portion of the rift is generally only 1-3 km wide. 2) The rift area rocks are generally (but irregularly) magnetic from 0-10 km north of Pahoa. (3) Basalt and dike rocks are generally weakly magnetic along the Chain of Craters between Iilewa Crater and Kapoho Crater, including the HGP-A, KS-1, KS-2 area. There is a strong suggestion of north-south structures which cut across the dominant east-northeast contour trend common to much of the rift zone. Plate III and the magnetic model interpretation should be studied for more detailed observations.

Electrical Studies

A large and somewhat confusing electrical data base is available for the east rift area (Keller et al., 1977). Several different methods have been used to obtain electrical resistivity (or conductivity) data on both reconnaissance and detailed scales and to minimize problems of high electrode impedances and conductive sea water. Most of the work has been done by a highly competent team of geophysicists. The work may have been somewhat limited by academic objectives (method comparisons, thesis study requirements) and by constraints of institutional and NSF funding. The main data sets are summarized here, and discussed in detail comparable to their importance to future geothermal exploration in the east rift zone. The more relevant data

have been replotted at an appropriate scale (1:100,000) to correspond to other data base items for this project. An integrated summary and critique of the data with recommendations follows.

Reconnaissance Dipole Mapping Surveys (Keller et al., 1977). A large, low frequency current was transmitted into the earth between current electrodes a large (1-3 km) distance apart. The voltage drop measured by orthogonal pairs of short (100-300 m) receiving electrodes in the vicinity of the source bipole are related to earth resistivities in the vicinity of the source, the receiver and the intervening earth. The receivers farther from the transmitting bipole are more strongly affected by the resistivity of rocks at depth, i.e. see deeper. Because of the complex interdependence of the received voltage on source and receiver sites, depth, and subsurface geometry, the data can be interpreted in a general manner only, and the true positions of resistivity discontinuities in depth or lateral position must be determined by other methods. A horizontally layered earth, resistive over conductive, would be expressed as an elliptical to dipolar shaped series of apparent resistivity contours which become lower in value farther away from the transmitter bipole. Keller et al. (1977) provide an exhaustive description (89 pages) of the data for 13 source bipoles, and approximately 200 receiver sites in the Kilauea - east rift zone - Puna area and of interpretational results.

The data for thirteen sources which cover most of the prospective geothermal area have been replotted at 1:100,000 on Plate IVA and IVB. The calculated apparent resistivity is normally plotted at the receiver site to avoid confusion, although it more meaningfully applies to the midpoint of the source-receiver area. Plates IVA and IVB present the contoured apparent

resistivity values from alternate sources to minimize the confusion due to overlapping coverage. Attempts to contour the data reveal the depth penetration and bipole source area dependence, and a distinct set of contours are produced for each bipole source. The departure of this pattern from the elliptical pattern of a layered earth can be used to identify areas of higher or lower resistivity for a given depth penetration. Several anomalous areas are indicated by Plate IV. High near-surface resistivities overlying lower resistivities are indicated near sources 4, 1, 6, 11, 3, 12, and 9. Lower resistivities are noted at shallow depths by sources 2, 5, 7, 8, and 10. Note the strong source resistivity dependence of S10 where low sea water resistivities dominate all resistivity values from this source.

Areas of overlapping coverage with consistent results (low or high resistivity) may sometimes be accepted as true resistivities for a given depth in these source areas, as at HGP-A (sources S2, S7) and between S9-S2-S10. The boundaries of the low resistivity areas cannot be defined without a substantial effort in computer modeling. Low resistivity areas in the Pahoa area are noted on the detailed electrical data summary, Plate V.

In summary these reconnaissance resistivity data indicate several poorly defined areas of low (2-10 ohm-m) resistivity at depths less than 1 km in the east rift zone area. The low resistivity effect of a sea water current path at ambient temperature (26°C) is indicated by 1-1.6 ohm-m resistivities at S10 stations. In the course of completing this review, problems were noted with: very high electrode impedances due to fresh water flushed, high porosity volcanic flows; numerous power lines and grounded structures which redistribute the input electrical current and act as independent current sources, thus confusing observed data values and the subsequent interpretation.

Resistivity Sectioning Surveys (Keller et al., 1977). A pole-dipole modification of the bipole-dipole array was used to determine apparent resistivities in line with and extending 150 m to 1250 m from either end of a 2 km bipole source. This work provided resistivity-versus-depth sections for three sections in the east rift: between Kaimu and Pahoa, and along the north side of the rift near Kapoho crater. The sections are reproduced on Plate V. The authors note that depth penetration of the resistivity sectioning is limited to about 600 m, hence probably well above reservoir depths. These data show low resistivities (<5 ohm-m) at about 600 m within the rift and probable 2 ohm-m resistivities at depths approaching 1000 m near Kapoho Crater. The data are interpreted only qualitatively, so these depths and intrinsic resistivities should be considered approximate.

Time-Domain Electromagnetic (TDEM) Survey, East Rift Zone, Kilaueau (Keller et al., 1977; Skokan, 1974). This TDEM survey was completed in 1974 using a 2.5 km line source and a 305 m loop of 26 conductor cable laid out as a square. A square wave of 15-sec period introduced between 5- and 15-amps of current into the ground and the transient magnetic field was measured with the receiving loop. Interpretation in terms of earth resistivity was made thru curve matching techniques. These data supplement the reconnaissance dipole-dipole survey, and are most useful as interpreted cross sections (pg. 85, Fig. 57, Keller et al.). A general agreement with resistivity data is noted but both lack position detail.

Electromagnetic Induction Sounding Measurements, Puna District, (Kauahikaua and Klein, 1977). Variable frequency inductive sounding measurements were taken with a horizontal coplanar two-loop configuration in the lower east rift area. The effective depth of penetration of these 26

soundings was thought to be less than 200 m, much shallower than the geothermal resource. Mutual impedance data were obtained for the frequency range 20 Hz to 10 KHz for each of 29 inductive soundings, and compared to the results of Schlumberger soundings. Five of the 29 inductive soundings were not interpretable in terms of layered earth models. The soundings indicated a highly resistive (>20,000 to 2,500 ohm-m) overburden underlain by a more conductive zone (salt water). Several soundings were able to define the fresh water - salt water interface where present, or the depth to the saline water table. These data contribute relatively little to the definition of the geothermal system, and have not been replotted as an overlay to other data bases.

Electromagnetic Transient Soundings, East Rift Area (Kauahikaua and Klein, 1977). This constitutes the most important detailed data set for the lower east rift area of Kilauea. The survey method and a preliminary interpretation are reported in detail (Kauahikaua and Klein, 1977) with a more complete numerical interpretation reported later (Kauahikaua, 1981). This survey employed a finite length (400m - 1.4 km) horizontal line source with step function current variation. The magnetic field resulting from this source induces secondary electrical currents in conductive zones. The amplitude and decay rate of the secondary currents are a function of the earth's local resistivity structure. The method can be used to advantage for resistivity profiling when high electrode impedances pose difficulties for the grounded electrode d.c. resistivity methods. As used here, 20 to 40 steel stake electrodes were required at each end of the source. A 15-KVA generator provided a constant 1000V signal resulting in 2A to 6A maximum current. The half-period of the transmitted signal was 8.5 seconds. The receiver was a 42 turn square coil enclosing about 5800 m^2 (76 m on a side).

The survey consists of 24 soundings about four different sources in a 50 square km area. Only 17 soundings were interpreted as a layered earth resistivity model, and these interpretations are summarized in Plate V. Depths to the second (conductive) layer range from 250 m to 1300 m below sea level. The 17 soundings are insufficient to provide a reliable resistivity contour map and there is considerable ambiguity between thickness and resistivity in parameter resolution. Nonetheless the data do indicate a low resistivity ($\sim$2 ohm-m) zone which probably includes the HGP-A well and Puu Honuaula crater area. Kauahikaua concludes that the low resistivities at depths of 1 km could not be explained by increased porosity (containing sea water) alone, and must result from water temperatures of 200-250°C. The TDEM soundings represent good reliable data for a small part of the east rift area. A minimum of 40 additional soundings would be necessary for an adequate delineation of geothermal resource potential in the Puna area.

Mise-à-la-masse survey, HGP-A (Kauahikaua et al., 1980). Kauahikaua and co-workers conducted a mise-à-la-masse survey about HGP-A using the drill casing as an electrode. From this survey they interpret a local zone of higher resistivity, 10-20 ohm-m, immediately adjacent to HGP-A, surrounded by lower resistivity (2 to 5 ohm-m) zones. They further interpret this as a compartment of dike-impounded fresh water surrounded by seawater-saturated rock. Their interpretation is in general agreement with the geologic-hydrologic model envisioned for the rift zone and with the HGP-A well log interpretation of Rudman (1978). The contoured electric potentials about the well are observational fact and clearly indicate two things. The dominant effect of high current density around the casing and high near surface resistivity are indicated by the strong circular contours close to the well. The definite rectangular elongation of contours at distances greater than 0.8

km from the well do indicate the northeast-southwest structural orientation and fluid distribution along the rift.

The apparent resistivity contours must be considered as estimates subject to considerable error since the current density decreases with depth along the casing, especially below the water table depth of 200 m. In addition the casing below 670 m is still a preferential current path even though not mechanically continuous with casing above the break. Thus there are some inaccuracies in the actual computation of apparent resistivity values, which I am sure the authors recognize. We note that Rudman (1978) reports low resistivities, generally 2.5 to 8 ohm-m from 2230 to 3450 feet (680-1052 m). The resistivity model they present (Fig. 3, their report) must also be considered approximate. A more exact numerical interpretation of the author's data is now possible with computer programs under development at ESL/UURI, but an exact numerical representation of the current source is not yet possible. Detailed dipole-dipole profiles perpendicular to the rift zone and either side of HGP-A would offer a much more accurate resistivity model for depths of 0 to 1000 m. The difficulty of completing such work has already been discussed.

The apparent resistivity data of this survey are considered too detailed, different in nature, and approximate for inclusion in Plate V. The data do have a high value for future more detailed interpretation however.

Resistivity Summary. As a result of the various electrical surveys, five areas of low electrical resistivity were delineated as shown in Figure 3. Area A (Pahoa anomaly) includes the HGP-A, KS-1, and L-1 wells. Area B, also known as the Opihikao anomaly, is believed to include conductive rocks at depths of 700 to 1200 meters (Furumoto, 1976). Areas C and D have not been tested at depth. Low resistivity values at area E have been attributed to

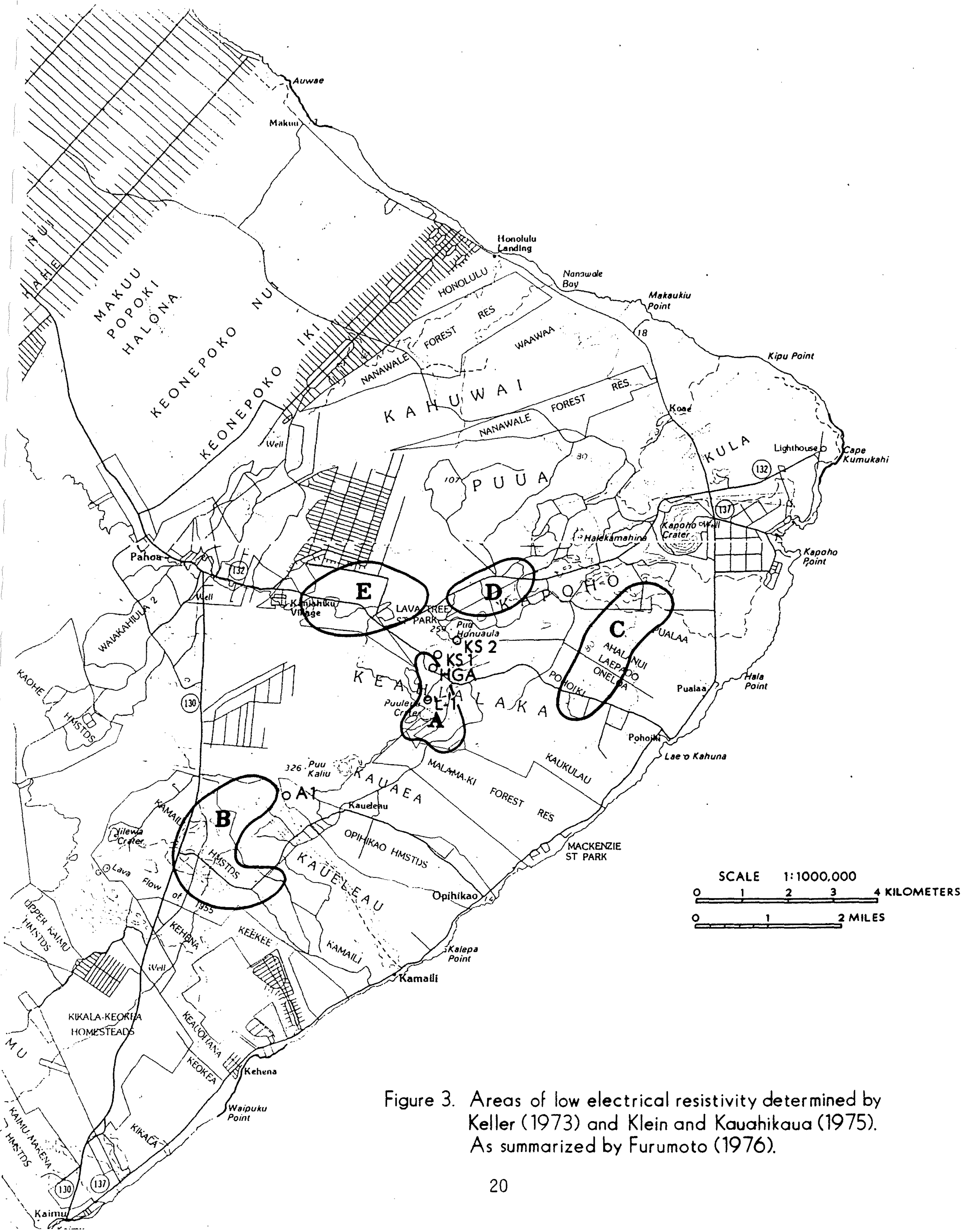

Figure 3. Areas of low electrical resistivity determined by Keller (1973) and Klein and Kauahikaua (1975). As summarized by Furumoto (1976).

grounded structures such as buried pipes and cables and has not been pursued as an exploration target area.

Plate V presents a summary of essentially all the detailed electrical data for the Puna geothermal resource area. Interpreted geoelectric sections corresponding to peripheral areas (after Keller et al., 1977) are also shown. The low resistivity zone determined for the integrated data base is plotted here. The low resistivity zones of Figure 3 are included in the broader regions indicated on Plate V. Low resistivity zones thought to be due only to salt water intrusion were eliminated from Figure 3 resulting in substantially smaller target areas. We are uncertain as to the accuracy of this refinement.

Self-Potential (SP) Survey, East Puna Area, Hawaii (Zablocki, 1977). The self-potential data indicate the presence of electrical potentials rather than the resistivity distribution. Natural electric currents can result from the differential movement of ions in thermal waters (electrokinetic mechanisms) or thermoelectric effects present in geothermal areas. Corwin and Hoover (1979), Fitterman (1979), and Sill (1982) have made recent contributions to understanding the SP phenomena as it occurs in geothermal systems. Zablocki (1977) has mapped four positive SP anomalies within the rift zone which are superimposed on a regional topographic streaming potential. Zablocki proposes a thermokinetic (streaming potential) origin for anomalies A, B, C, and D and indicates that the potentials probably arise from selective ion displacement in the pore fluids by temperature and/or pressure gradients. Zablock's (1976) earlier self-potential studies on Kilauea, also shown on Plate VI, indicated a close spatial association between the SP anomalies and local heat sources. Anomaly C on Plate VI includes the successful geothermal well HGP-A, and is

likely a result of convective geothermal fluid movement in this area.

Dr. W. R. Sill has reviewed Zablocki's study, and completed a quantitative evaluation of the 400 millivolt anomaly A, which is approximately two-dimensional (Appendix I). Using reasonable values for the streaming potential coefficient, permeability, and conductivity, and estimating a maximum velocity resulting from a maximum temperature change of 200°C, Sill calculates a self-potential anomaly of about 200 mv. This is only one-half the observed anomaly (A), but certainly lends credence to Zablocki's interpretation of the convective source mechanism. Drill results at HGP-A, near anomaly C, indicate that the source temperature may be substantially greater than the 200°C Sill assumed. The complex three-dimensional nature of SP anomalies B and C, although geologically encouraging, are less suited to mathematical simulation. The order-of-magnitude agreement between observation and model results for anomaly A give support to a convective source for all the identified SP anomalies, A, B, C and D.

Seismic Data

The seismic data base for the east rift area is also varied and extensive. Most of the relevant data are reported and interpreted in a single report of the Hawaii Institute of Geophysics, HIG-78-8, by Suyenaga et al. (1978). The ongoing record of earthquake activity has been reported quarterly and annually by the USGS. Suyenaga and Furumoto (1978) present a summary of earthquake epicenters for the period 1964-1973 which indicates the non-specific distribution of larger magnitude earthquakes ($m > 2.5$) in the entire east rift area. The earthquake epicenters, shown on Plate VII, indicate that the major seismicity results from the east rift tectonic processes rather than the geothermal system itself. A similar observation is forthcoming from the

microearthquake surveys.

Microearthquake Surveys

Suyenaga and Furumoto (1978) also report the results of a microearthquake survey with a seven seismometer array which was conducted for a short (three week) period during the summer of 1974. They observed that: 1) most earthquakes occurred within a three-km band vertically beneath the rift zone; 2) many hypocenters occur along a plane about five km deep which extends from HGP-A four km to the north-northwest; 3) high velocity material continues through the entire rift zone, and coincides roughly with the gravity maximum over it; 4) there is a noticeable lack of activity in the rift zone northeast of Puu Honuaula, suggesting a possible discontinuity in the rift zone at Puu Honuaula. Plate VII shows a dominant north-south trend of epicenters 1-3 km deep which cuts through a low resistivity area (ER) and terminates the high resistivity area (HIR) on the east (Plate VIII). Few epicenters are located in the high resistivity area, and these are generally deeper, i.e. 5, 7, and 9 km. Ninety percent of the located epicenters occur in a three km wide north-trending band or a three km wide band along the trend of the rift.

Mattice and Furumoto (1978) report the results of a two station, twenty day microearthquake survey of the Opihikao resistivity-SP anomaly (Plate VII). They noted a high spatial coincidence of the earthquake epicenters and the electrical anomalies. Because only two stations were operating two possible source locations were possible for each event, and the data are best presented as an earthquake density or frequency of occurrence per unit area (PLate VII). The symmetric contour pattern suggests the earthquakes detected are those close to the two station net, rather than indicating a specific geologic feature. The limited area covered, and the inability to locate

specific epicenters limit the value of these data in reservoir delineation.

Seismic Ground Noise Survey

Norris and Furumoto (1978) conducted a seismic ground noise survey. Seismic noise for the frequency band 1-30 Hz was recorded at 59 stations for an average period of 10 minutes. The survey covered about 30-40 square miles in the Pahoa-Kapoho-Kalapana triangular area. The recording periods were extended if a significant level of ground noise was observed. They noted that no ground noise high was present near HGP-A, and concluded that ground noise, as surveyed, was not spatially related to hydrothermal activity on the east rift of Kilauea. Similar conclusions have been reached regarding ground noise surveys for several basin and range geothermal systems.

Seismic Refraction Surveys

Suyenaga (1978), and Broyles and Furumoto (1978) describe seismic refraction surveys in the east rift area and their interpretation as a model of crustal structure. Suyenaga describes two short reversed refraction lines with shot-receiver distances of 0.5 to 5 km. Four to 16 pound charges of Aquagel were detonated at depths of about 15 feet. Very poor first arrivals were noted at distances greater than 3 km but charge size could not be increased due to safety considerations and nearby houses and cultural features. The survey defined this near surface velocity model: depth 0-200 m, v = 0.7 to 1.3 km/s; depth 130-200 m, v = 2.5-3.1 km/s; depth 200-500 m, v = 2.9 to 3.1 km/s. The low near surface velocities were attributed to interlayered aa and pahoehoe lava flows with large voids within and between flows. The higher velocity (2.5-3.1 km/s) second and third layers mainly reflect water saturation at the water table rather than lithologic changes (Suyenaga, 1978). Shot-to-receiver distances greater than 4 km, requiring

larger explosive charges, would be required to detect the high velocity layer at depths greater than 500 m.

Broyles and Furumoto (1978) report two refraction profiles (XX' and YY', Plate VII) where 60 and 120 lb charges were detonated at sea. Shot-to-receiver distances of six to 24 km were used which permitted the mapping of the deeper (2-10 km) high velocity (7.0, 7.1 km/s) bodies associated with the inferred dike complex and basal volcanic flows.

The generalized velocity model resulting from these studies is reproduced on Plate VIII. The model portrays a velocity section across the rift through the Kalapana-Pahoa area which is seven km or more west of the actual observational data. The general configuration of the model, the velocities, and the average depth to the top of the dike complex, 2 to 2.5 km result primarily from the refraction data. The bottom of the dike complex is placed at five km depth on the basis of earthquake and microearthquake hypocenter plots, and to agree with geologic inference tying this depth with the magma chamber of Kilauea. The apparent north dip (6° to 9°) of the dike complex is derived in part from gravity data which I believe is ambiguous at this level of interpretation. The subsurface lateral width of the dike complex is also due in part to an ambiguous gravity interpretation. The thick, extensive 5.25 km/s layer is observed only on the north-south line (Y-Y') in contrast to the 7.0 km/s velocities at these depths on the east-west line (X-X'). An anisotropy of higher velocity along (as opposed to across) the dike complex seems a logical explanation for this disagreement. The argument that the 5.25 km/s layer may lie principally within the hydrothermal zone surrounding the geothermal reservoir (Broyles and Furumoto, 1978) is not well illustrated on the velocity section, and is somewhat speculative in view of the distribution

of the seismic array.

The refraction data are appropriate for velocity structure and a regional velocity model, but have not contributed to the definition of the geothermal system. Important conclusions of the refraction work are: 1) the depth to the top of the intrusive complex averages 2 to 2.5 km, but may be as little as 1 km locally; 2) the subsurface lateral extent of the rift complex is 12 to 19 km, much wider than indicated by surface features. The depth to the dike complex is probably more accurate than determined by any other data set to date, but may be improved by a detailed magnetic survey.

Furumoto (1978) brings many aspects of the refraction and passive seismic data together in an integrated interpretation. He believes that microearthquake data define a region of 6 km^3 about HGP-A that corresponds to the geothermal reservoir. This review suggests the microearthquake distribution has been largely determined by the seismometer array location and the limited recording period of the surveys. It seems premature to assign a size to the thermal reservoir on the basis of these data. Furumoto believes that tensional forces are produced by an expanding rift zone due to forceful intrusion of magma from the summit holding reservoir. Fractures form over the hot dike complex, and groundwater seeping into the fractures is trapped by a self sealing process to form the geothermal reservoir. Such an interpretation seems consistent with the large body of observational data.

DISCUSSION

The principal geophysical data sets have been presented, referenced and discussed individually. The interrelationships of these data and their relationship to the geothermal reservoir should be discussed in more detail.

Historical seismicity, microearthquake surveys, triangulation and leveling surveys confirm geologic observations that the south side of the east rift zone is the active area of rift development. This probably reflects the recent rise of magma and the continuing formation of the dike complex. The cooling magma and dike complex provide the heat for the geothermal reservoir. Abundant precipitation (100-200 inches per year) falls upslope from the east rift zone, and readily moves through porous near surface rocks to the top of the fresh water table. The fresh ground water moves down dip through porous and permeable basalt layers, above the deeper salt water interface, until ponded in the subsurface by the east-northeast trending dike complex.

The trend of the east rift zone is indicated by many faults, fractures, steaming fissures and other geologic features. The central portion of the rift coincides with the northeast trending elongate maximum of gravity data, but is not sharply defined by these data.

Regional aeromagnetic data indicate a more complex geology of the rift zone, including a possible transform fault near HGP-A which is also suggested by the detailed gravity data and microearthquake epicenters. A relatively narrow (1-3 km wide), strong, magnetic source corresponds to the southern edge of the rift zone between the Chain of Craters area and Iilewa Crater. The dike complex becomes weakly magnetic east of Iilewa Crater, and appears to be cut by north-south structural (or nonmagnetic) zones. Local areas which appear weakly magnetic may be near the Curie temperature ($\sim$ 580°C) closer to the surface, but this interpretation is somewhat speculative. A large, irregular, magnetic source is present north of Pahoa and north of Kapoho Crater. The magnetic data indicate a complex geologic setting not apparent in

other data sets.

A limited temperature data base suggests that heat sources are limited to the rift zone itself. This is likely to be the case but few wells penetrate the cold water recharge zone north of the rift zone and no deep well temperatures are available south of the rift zone and west of Highway 130. Several self-potential maxima appear to arise from convective heat flow and thermokinetic effects, and are spatially associated with the geothermal reservoir(s). Zablocki's anomalies B and C (Plate VI) nicely portray the intersection of the rift zone itself and the probable north-south trending transform fault. Low apparent resistivities occur at depth throughout much of the east rift zone due to salt water below sea level in the porous basalt flows. Resistivities as low as 2 ohm-m require anomalously high fluid/rock temperatures, as mapped at the HGP-A reservoir area. The electrical resistivity data base, although extensive, is not of adequate density or detail to delineate the geothermal reservoir(s). High impedance surface electrodes essentially preclude a high quality detailed electrical resistivity data base because of the high costs of data acquisition.

Plate VIII attempts to summarize the more important data sets which help delineate the geothermal reservoir and other areas of geothermal potential. The geothermal potential seems to be reasonably well identified at this scale (1:100,000).

A typical scale for advanced exploration of a geothermal resource or major mineral deposit is 1:24,000. Plate IX illustrates some of the detailed data at this more appropriate scale. It is clear that the geothermal reservoir is not adequately defined by the detailed electrical data or well tests.

SUMMARY AND RECOMMENDATIONS

The compilation of public geophysical data for the Kilauea east rift zone has been completed at a scale of 1:100,000. The known geothermal resource is well expressed as a maximum in the self-potential data and as one of several resistivity lows in the electrical resistivity data base. Regional aeromagnetic data indicate a complex geologic structure for the east rift zone that is not apparent in the gravity or regional resistivity data. I conclude that a detailed, low level aeromagnetic survey offers the most promise for defining the subsurface structural features (and possibly the gross temperature distribution) of the east rift zone in a cost effective manner. The subsurface temperature data base is limited to a small portion (Puna area) of the east rift zone, and the self-potential data base is also incomplete.

The HGP-A geothermal reservoir appears to be localized by the intersection of the center of the rift zone and a north-northwest trending structure, probably a transform fault. The structure is indicated by gravity, aeromagnetic, microearthquake and self-potential data. This reservoir is not well delineated by the resistivity data due to numerous problems in obtaining detailed electrical resistivity data in this volcanic environment.

Although the HGP-A area appears to be the most promising setting for a geothermal reservoir, based on the existing data, a resistivity (B) and self-potential anomaly (A) seven kilometers southwest of HGP-A also seems promising. Other geothermal reservoirs may be present but not clearly indicated because of the irregular distribution of electrical resistivity, self-potential and well temperature data.

A detailed, low level aeromagnetic survey is recommended as the highest

priority for further exploration. Such a survey offers the possibility of determining the position and geometry of structural features and relative magnetizations along the rift. Suggested survey parameters are: 1) line spacing no greater than 400 m in the Puna area but as much as 800 m for areas to the west; 2) a smoothly draped flight path between 200 and 300 meters above mean terrain level; 3) flight direction north-south or northwest perpendicular to the rift; 4) several tie lines along the trend of the rift to closely define irregularities within the rift itself.

Acquisition of additional (proprietary) geophysical data may well be cost effective if the duplication with existing data is not great, and the data are of good quality. It is apparent that all roads and trails of even marginal accessibility have been considered for ground electrical work (resistivity and self-potential) and acquiring new survey data without reasonable access will be both costly and slow. Pending a review of available proprietary data and detailed aeromagnetic data, preferably at a scale of 1:24,000, the cost effectiveness of new surveys should again be evaluated. Controlled source audiomagnetotelluric (CSAMT) may be a cost-effective technique for mapping the low resistivity second layer in detail, but the expected responses should be numerically modeled prior to undertaking new surveys.

Seismic refraction surveys have provided a useful regional velocity model and the best estimates to the top of the dike complex. In a conceptual sense one would like to map the detailed velocity structure including and surrounding the geothermal areas. In practice this would be difficult to carry out, would require large receiver arrays and should be considered high risk in terms of results versus costs. Shot-to-receiver distances of 5 to 15 km would be required for velocity mapping for depths of one to two km. This

would probably require charges greater than 10 pounds of Aquagel, based on Suyenaga's experience, and would dictate offshore or remote area shot locations. There may be some merit to considering refraction fan arrays in hopes of determining small velocity lags near the geothermal sites which could be interpreted in terms of fracturing or alteration. Any additional refraction surveys should be given a lower priority than the proposed detailed magnetic survey and the acquisition of proprietary resistivity data.

There is much interest in determining the total power production potential for the east rift zone to facilitate economic planning. Present estimates of the lateral extent of the reservoir, based on microearthquake data must be considered premature and subject to considerable error. It is apparent that maps of microearthquake epicenter locations and density (i.e. Plate VII) are heavily biased by the location and extent of the seismograph net and the limited period of observation for the data reviewed here. A geometric definition of the reservoir through magnetic and resistivity data, integrated with multiple well production test results is required to determine the power generating potential of the known geothermal reservoir.

REFERENCES

Broyles, M. L., Suyenaga, W., and Furumoto, A. S., 1978, Structure of the lower east rift zone of Kilauea Volcano, Hawaii from seismic and gravity data: Jour. of Volcanology and Geothermal Research, v. 5, p. 317-336.

Broyles, M. L., and Furumoto, A. S., 1978, Crustal structure of the lower east rift zone of Kilaueau, Hawaii from seismic refraction. 2. Complete structure in HIG-78-8, p. 93-122.

Corwin, R. F., and Hoover, D. B., 1979, The self-potential method in geothermal exploration: Geophysics, v. 44, p. 226-245.

Epp, D., and Halunen, A. J., Jr., 1979, Temperature profiles in wells on the island of Hawaii: HIG Report HIG-79-7, 31 p.

Fitterman, D. V., 1979, Calculations of self-potential anomalies near vertical contacts: Geophysics, v. 44, p. 195-205.

Furumoto, A. S., 1978, Nature of the magma conduit under the east rift zone of Kilauea Volcano, Hawaii: Bull. Volcanol., v. 41-4, p.1-19.

Furumoto, A. S., 1978, Thermal processes of Kilauea east rift inferred from seismic data: in HIG-78-8, p. 123-137.

Furumoto, A. S., Norris, R., Kam, M., and Fernander, C., 1976, Gravity profile and the intrusive zone: Hawaii Geothermal Project Initial Phase II Prog. Rep., Univ. Hawaii, p. 26-31.

Furumoto, A. S., 1976, A coordinated exploration program for geothermal sources on the island of Hawaii: in Proc. of the Second U. N. Symposium on the development and use of geothermal resources, San Francisco, CA, May 1975, v. 2, p. 993-1001.

Furumoto, A. S., and Korack, R. L., 1979, The Kalapana earthquake of November 29, 1975: An intra-plate earthquake and its relation to geothermal processes: Physics of the Earth and Planetary Interiors, v. 18, p. 197-208.

Godson, R. H., Zablocki, C. J., Pierce, H. A., Frayser, J. B., Mitchell, C. M., and Sneddon, R. A., 1981, Aeromagnetic map of the island of Hawaii: USGS Geophys. Investigations Map GP-946.

Hawaii Institute of Geophysics, 1982, Geothermal Resources of Hawaii: Map produced by National Geophysical Data Center, NOAA.

Holcomb, R. T., 1980, Preliminary geologic map of Kilauea Volcano, Hawaii USGS Open File Report.

Kauahikaua, J., and Klein, D., 1978, Results of electrical survey in the area of Hawaii geothermal test well HGP-A: Geothermal Resources Council Trans., v. 2, p. 363-366.

Kauahikaua, J. P., and Klein, D. P., 1977a, Electromagnetic induction sounding measurements, in HIG-77-15, p. 91-120.

Kauahikaua, J. P., and Klein, D. P., 1977b, Interpretation of electromagnetic transient soundings made on the east rift of Kilauea Volcano, Hawaii: in HIG-77-15, p. 121-174.

Kauahikaua, J., 1981, Interpretation of time-domain electromagnetic soundings in the east rift geothermal area of Kilaueau Volcano, Hawaii: USGS Open File report, 81-(draft version), 17 p.

Kauahikaua, J., Mattice, M., and Jackson, D., 1980, Mise-à-la-masse mapping of the HGP-A geothermal reservoir, Hawaii: Geothermal Resources Council Trans., v. 4, p. 65-68.

Keller, G. V., Skokan, C. K., Skokan, J. J., and Daniels, J., 1977b, Electrical resistivity and time-domain electromagnetic surveys of the Puna dn Ka'u districts, Hawaii County, Hawaii: in HIG-77-15, p. 1-90.

Keller, G. V., Skokan, C. K., Skokan, J. J., Daniels, J., Kauahikaua, J. P., Klein, D. P., and Zablocki, C. J., 1977a, Geoelectric studies on the east rift, Kilauea Volcano, Hawaii island: HIG report HIG-77-15, 195 p.

Kinoshita, W. T., Krivoy, H. L., Mabey, D. R., and MacDonald, R. R., 1963, Gravity Survey of the island of Hawaii: USGS Prof. Paper 475-C, p. C114-C116.

Krivoy, H. L., and Eaton, J. P., 1961, Preliminary gravity survey of Kilauea Volcano, Hawaii: Art. 360 in USGS Prof. Paper 424-D, p. D205-D208.

Macdonald, G. A., 1949, Petrography of the island of Hawaii: USGS Prof. Paper 214-D, 96 p.

Malahoff, A., and Wollard, G. P., 1968, Magnetic and tectonic trends over the Hawaiian ridge: Am. Geophys. Union Geophys. Mon. 12, p. 241-276.

Mattice, M. D., and Furumoto, A. S., 1978, Microearthquake study of the Opihikao anomaly, Puna, Hawaii: in HIG-78-8, p. 41-56.

Moore, J. G., 1971, Bathymetry and geology-East Cape of the Island of Hawaii: USGS Misc. Inv. Map I-677.

Moore, R. B., 1982, Preliminary geologic map of the Pahoa South quadrangle, Hawaii: Open File report.

Norris, R., and Furumoto, A. S., 1978, Seismic ground-noise survey, Puna, Hawaii: in HIG-78-8, p. 57-78.

Peterson, D. W., 1979, Geologic map of the Kilauea Crater Quadrangle, Hawaii: USGS Map GQ-667.

Rudman, A. J., 1978, Analysis of geophysical logs from the Hawaii geothermal project well: Hawaii Inst. Geophysics report HIG-78-9, 25 p.

Sill, W. R., 1982, Self-potential effects due to hydrothermal convection (velocity cross coupling): Dept. of Geology and Geophysics, Univ. of Utah, DOE Report DOE/ID/12079-68.

Suyenaga, W., 1978, Crustal structure of the east rift zone of Kilauea, Hawaii from seismic refraction: 1. near surface structure in HIG-78-8, p. 79-92.

Suyenaga, W., Broyles, M., Furumoto, A. S., Norris, R., and Mattice, M. D., 1978, Seismic studies on Kilauea Volcano, Hawaii island: Hawaii Inst. Geophysics report HIG-78-8, 137 p.

Suyenaga, W., and Furumoto, A. S., 1978, Microearthquake study of the east rift zone of Kilaueau, Puna, Hawaii: in HIG-78-8, p. 1-40.

Swanson, D. A., Duffield, W. A., and Fiske, R. S., 1976, Displacement of the south flank of Kilaueau Volcano: the result of forceful intrusion of magma into the rift zones: USGS Prof. Paper 963, 39 p.

Thomas, D., Cox, M., Erlandson, D., and Kajiwara, L., 1979, Potential geothermal resources in Hawaii: A preliminary regional survey: Hawaii Institute of Geophysics report, HIG-79-4, 103 p.

Zablocki, C. J., 1976, Mapping thermal anomalies on an active volcano by the self-potential method, Kilauea, Hawaii: in Proc. of the Second U.N. Symposium on the development and use of geothermal resources, San Francisco, CA, May 1975, v. 2, pp. 1299-1309.

Zablocki, C. J., 1977, Self-potential studies in East Puna, Hawaii: in HIG-77-15, p., 175-195.

APPENDIX I

SELF-POTENTIAL STUDIES IN EAST PUNA, HAWAII

(by C. J. Zablocki)

Memorandum from W. R. Sill to H. P. Ross, Aug. 12, 1982

UNIVERSITY OF UTAH RESEARCH INSTITUTE

UURI

EARTH SCIENCE LABORATORY
420 CHIPETA WAY, SUITE 120
SALT LAKE CITY, UTAH 84108
TELEPHONE 801-581-5283

August 12, 1982

MEMORANDUM

TO: H. P. Ross

FROM: W. R. Sill

SUBJECT: Self-potential Studies in East Puna, Hawaii by C. J. Zablocki

In the above paper Zablocki proposes a convective model for the self-potential anomalies as in Figure 1 (his Figure 4). In a recent report (Sill, 1982) I investigated the modeling of self-potential effects due to convection. Figure 2 shows the results for two models. In both models the maximum temperature (200°C) is the same as are the velocity fields. The maximum temperature and velocity are at $X = 0$, $Z = \beta^{-1}$ as indicated in the figure. The flow field is upward in the plume ($-a \leq x \leq a$) and the return flow takes place in the exterior region. As the figure shows, the self-potential reaches a maximum near the center of the plume and it is larger in the case where the cross coupling parameter (L) is zero exterior to the plume. The normalized potential (ϕn) in the model is related to the true potential (ϕ) by

$$\phi' = \phi_n L' V_o' \Delta x'/\sigma'. \qquad (1)$$

where L' = true velocity cross coupling parameter

V_o' = true convective velocity (maximum)

$\Delta x'$ = true length scale

σ' = true conductivity.

The velocity cross coupling parameter L is related to the better known streaming potential coefficient (C) by

$$L = \sigma C/k. \tag{2}$$

where k = permeability.

In order to scale the model results to any geological setting we have to estimate the true parameters in equation (1). The length scale ($\Delta x'$) can be estimated by noting that the anomaly width at the one-half amplitude points is around 3 to 4 model units. The one-half amplitude widths in Zablocki's report are in the range from 500 m to 600 m so the length scale is around 150 m to 200 m. The depth to the maximum temperature (200°C) and the maximum velocity in the plume is then around 300 m to 400 m. The estimates of the other parameters is simplified by making use of an approximate relation between the maximum temperature change Tm and the maximum velocity (V_0)

$$V_0 \tilde{=} \gamma \alpha g \, Tm \, k_0 \eta_0 / \eta(Tm). \tag{3}$$

where α = rate of change of water density with temperature

g = acceleration of gravity

k_0 = permeability at room temperature

η_0, Tm = Viscosity of water at room temperature, Tm

γ = shape factor for type of convection.

The shape factor γ varies from 1/2 for nearly equidimensional flows (horizontal length = vertical length) to values greater than 1 for flows with vertical length > horizontal length.

Making use of equations (3) and (2) in equation (1) and noting that parameters for the model are specified at room temperature, we get

$$\phi' = \gamma\phi_n \, C \, \alpha \, g \, Tm \, \Delta x' \eta_o/\eta(Tm). \qquad (4)$$

In equation (4) the parameters $\Delta x'$, Tm, γ have already been specified ϕ_n, α, g and $\eta_o/\eta(Tm)$ are known so the only free parameter is the streaming potential C. Typical values of C for rocks full in the range from 5 to 25 mv/atm (1 mv/atm = 10^{-8} MKS). Taking as a best case, model 2 (ϕ_n = .4) with C = 25 mv/atm we get an estimate for the self-potential (ϕ') of about 200 mv. Since the observed anomaly (Figure 1) is about 400 mv we fall short by a factor of two. The anomaly could be explained with C = 50 mv/atm but values this large are not typical of rocks. For model 1 the required streaming potential is around 100 mv/atm. One might be tempted to scale up Tm in equation (4) but the model results are not linear in temperature and the Tm used in equation (4) must be the same as that used in the calculation of ϕ_n. The results of this investigation indicate that the model suggested by Zablocki is in the gray area of plausibility. The required streaming potentials are very large compared to the typical values for rocks but then the model fit to the real situation is poorly known. A reduction in the required streaming potential could result from an increase in temperature but more likely from an increase in the shape factor γ. The latter should increase some if the flow has a thin plume with a large vertical scale. Estimating γ or the true V_o would involve the solution of the appropriate convection problem. In a "full up" solution of the convection problem the calculated velocity field can be used to model the self-potential by the technique presented in Sill (1982).

References

Sill, W. R., 1982, Self-potential effects due to hydrothermal convection (velocity cross coupling), Dept. of Geology and Geophysics, University of Utah, DOE Report DOE/ID/12079-68.

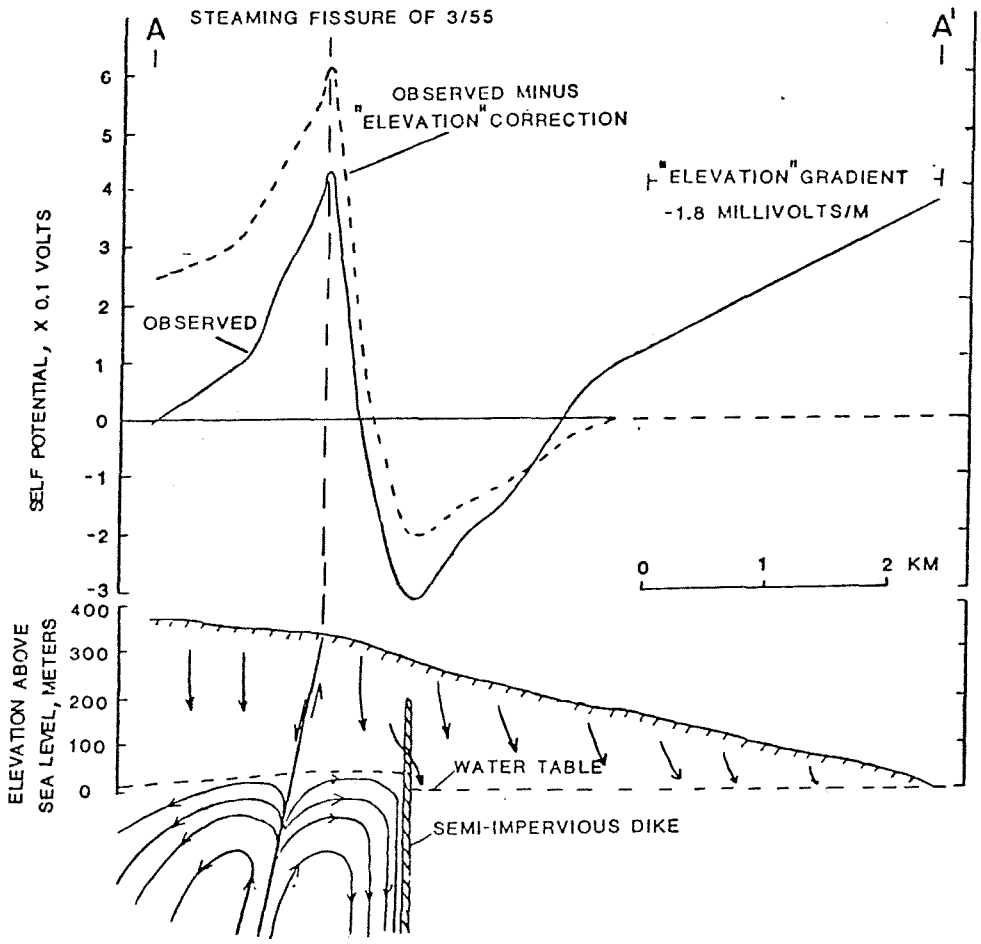

Figure ~~X~~ 1 Self-potential profile (solid) along traverse A-A' (Fig. 2) and modified profile (dashed) after removal of an "elevation" gradient. The cross section shown below the profile is a conceptual model of the hydrology and substructure that may account for the potential distribution as discussed in the text. Arrowed-lines below water table are idealized streamlines of fluid (liquid and vapor) flow, and above water table, are downward migration of meteoric water.

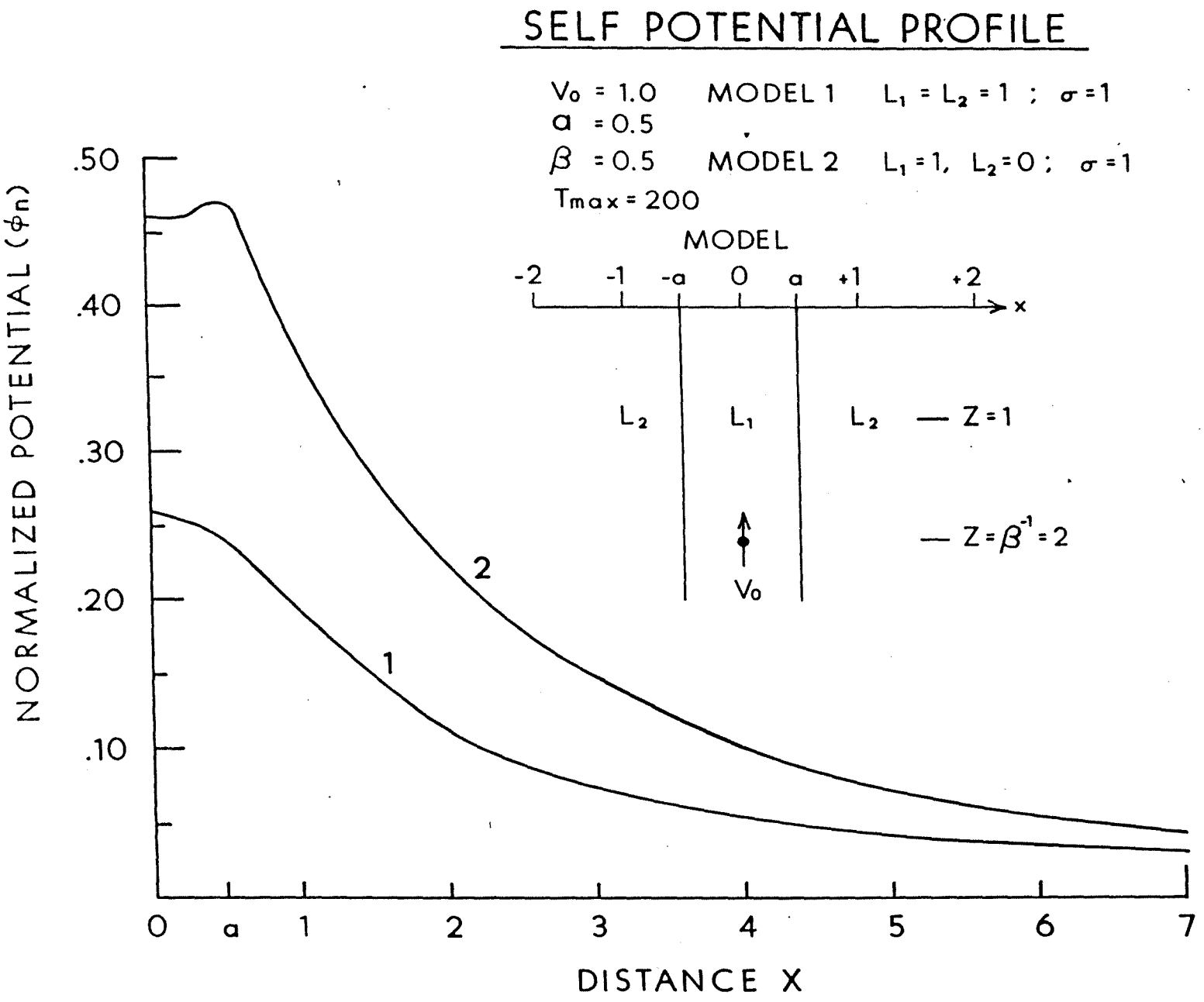
SELF POTENTIAL PROFILE
V_o = 1.0 MODEL 1 $L_1 = L_2 = 1$; $\sigma = 1$
a = 0.5
β = 0.5 MODEL 2 $L_1 = 1$, $L_2 = 0$; $\sigma = 1$
Tmax = 200
MODEL
-2 -1 -a 0 a +1 +2 x
L_2 L_1 L_2 — Z = 1
— $Z = \beta^{-1} = 2$
V_o
NORMALIZED POTENTIAL (ϕ_n)
.50
.40
.30
.20
.10
1
2
0 a 1 2 3 4 5 6 7
DISTANCE X

FIGURE 2

APPENDIX II

MAGNETIC MODEL INPUT PARAMETERS
(See Plate III B)

APPENDIX II

MAGNETIC MODEL INPUT PARAMETERS (See Plate III B)

Iter #3

Project name: EAST RIFT AREA
AMAG. MODEL

Model: MODEL A-I2

Units in Meters

X_1, X_2 = East-West coordinates (m)
Y_1, Y_2 = North-South coordinates (m)
D_1 = Depth below plane to top of body (m)
D_2 = Depth below plane to bottom of body (m)
SC = Magnetic susceptibility (cgs)

MAGNETIC PARAMETERS
Earth"s field: 35850. gammas.
Inclination = 37. degrees Declination = 11. degrees.

PRISM	X1	X2	Y1	Y2	D1	D2	DC	SC
1	12150.	18000.	300.	4800.	1000.	5000.	0.00	6000.
2	7900.	12150.	2800.	9400.	1000.	5000.	0.00	6000.
3	1500.	6300.	3800.	9700.	1000.	5000.	0.00	10000.
4	3000.	4400.	1000.	3800.	500.	2000.	0.00	6000.
5	-2300.	0.	-1000.	2600.	700.	5000.	0.00	6000.
6	-7600.	-2300.	-1000.	4500.	700.	5000.	0.00	6000.
7	-2300.	-1000.	-9100.	-7600.	500.	5000.	0.00	4500.
8	-5800.	-2300.	-9500.	-8100.	500.	5000.	0.00	9000.
9	-8300.	-5800.	-10400.	-8900.	500.	5000.	0.00	9000.
10	-11100.	-8300.	-11400.	-10100.	500.	5000.	0.00	9000.
11	-13100.	-9600.	-12600.	-11400.	500.	5000.	0.00	9000.
12	-18400.	-13100.	-14000.	-11500.	500.	5000.	0.00	9000.
13	8400.	9900.	-3600.	-2500.	700.	5000.	0.00	6000.
14	5100.	8400.	-4100.	-2200.	700.	4000.	0.00	8400.
15	1800.	5100.	-3400.	-1300.	700.	4000.	0.00	8400.
16	2800.	5700.	-6000.	-4800.	700.	5000.	0.00	6000.
17	4000.	8200.	9700.	11300.	1000.	5000.	0.00	6000.
18	-4300.	-2600.	-2400.	-1000.	700.	5000.	0.00	6000.
19	-1000.	4700.	-9600.	-6000.	700.	5000.	0.00	2000.
20	13800.	18400.	300.	1400.	1000.	3000.	0.00	-6000.